LA-8421-MS
Informal Report

UC-38
Issued: October 1980

The BDD: A Dosimeter for the Global Positioning System

Harold V. Argo
Daniel N. Baker
Richard D. Belian
Leroy K. Cope
Paul R. Higbie

master

THE BDD: A DOSIMETER FOR THE GLOBAL POSITIONING SYSTEM

by

Harold V. Argo, Daniel N. Baker, Richard D. Belian,
Leroy K. Cope, and Paul R. Higbie

ABSTRACT

This report describes the design and operation of the BDD, a four-channel spectrometer carried by some satellites of the Global Positioning System to collect data about magnetically trapped particle fluxes. The methods of data collection and analysis are also discussed.

I. INTRODUCTION

Satellites of the US Air Force Global Positioning System (GPS), which are in highly inclined (55-63°) circular orbits at an altitude of 11 000 nautical miles, pass twice per 12-h orbit near the peak-intensity region of magnetically trapped energetic particles. Radiation damage to the satellite components would be detrimental to the system's planned longevity. Available experimental or theoretical knowledge of particle fluxes at GPS orbits is inadequate for predicting the extent of radiation damage, largely because the resident trapped particle populations vary and, in addition, depend on the level of solar activity.

A secondary mission of the GPS program, beginning with the launch of the satellite FSV-6 in late 1980, is to carry instrumentation in support of the Integrated Operational Nuclear-Test Detection System program. This instrumentation includes an x-ray burst detector (BDX) and a logic-control and data-storage unit (BDP). It was decided that the simplest and most effective way to obtain the required particle-flux data is to equip some satellites with an appropriate dosimeter rather than a BDX. Because this decision was made when the BDP and the BDX were already in the hardware stage, restrictions were placed on the dosimeter (BDD) design.

- The shape, weight, and power requirements of the BDD were to be the same as those of the BDX.
- The BDD was to be connected to the BDP with the same cable that connects the BDX to the BDP.
- The BDD data format was to be fitted into the existing BDX data train stored in the BDP.

These requirements have been met with no change in the BDP hardware and with the addition of only a single hard wire to the connecting cable. The level on this wire determines the subset of BDP firmware appropriate to processing data from a BDX or a BDD.

II. DOSIMETER CONCEPT AND DESIGN

For the purpose at hand, the most useful form of dosimeter data is energy spectra with absolute intensity as a function of time and position in orbit. From such data one can calculate the radiation dose received by a satellite component and so predict the expected degradation of its performance with time. Within the design restrictions mentioned above, we have devised a four-channel spectrometer that will provide electron-flux data over the energy range from 0.3 to 10 MeV and proton-flux data from 6 to 100 MeV.

Figure 1 shows simplified sketches of the BDD package and detector geometry. A 700-μ-thick surface-barrier silicon sensor in each of the four channels is protected from the full radiation intensity by a thick hemispherical dome. Particles are admitted to the sensor through cylindrical, radially oriented collimating apertures in the dome. Thin hemispherical filters covering the bottoms of the collimating apertures determine the energy range covered by each channel. This "saltshaker" design permits the detectors to sample uniformly a large fraction of one hemisphere (and thus to measure the average omnidirectional flux) and at the same time shields the sensors from more than 99.2% of the incident particle flux.

The protective dome consists of an outer shell of aluminum (replaced at very low angles to the satellite surface by tungsten) and an inner shell of gold. The thickness of aluminum was chosen to stop electrons while minimizing bremsstrahlung from them. The gold was chosen to stop very energetic electrons since not enough space was available to use aluminum exclusively. The tungsten section provides a well-defined polar angle for calculating the response of the detector to particles that leak through the aluminum/gold shielding.

The diameters of the collimating apertures in each dome have been matched to the threshold energy of that channel so that the expected dose rates in all channels will be comparable.

The thin hemispherical filters, which determine the energy range of each channel, are of aluminum, iron, or tungsten. Equivalent aluminum thicknesses of 10, 25, 60 (21 mils of iron), and 135 (20 mils of tungsten) mils provide electron energy thresholds (measured) of 0.31, 0.57, 1.05, and 1.45 MeV, respectively, and proton energy thresholds of 6, 10, 17, and 27 MeV, respectively.

The four energy channels have been fitted onto the existing surface plate of the BDX unit; the associated power supply, amplifiers, discriminators, and data-processing logic have been fitted into the existing BDX container. Care was taken to position the collimating apertures so that they are not aligned with any satellite antennas or other fixtures occupying the same satellite face.

Table 1 lists various design parameters for the four channels of the BDD. The photograph of Fig. 2 shows the four detectors of the BDD; that of Fig. 3 shows the electronics package.

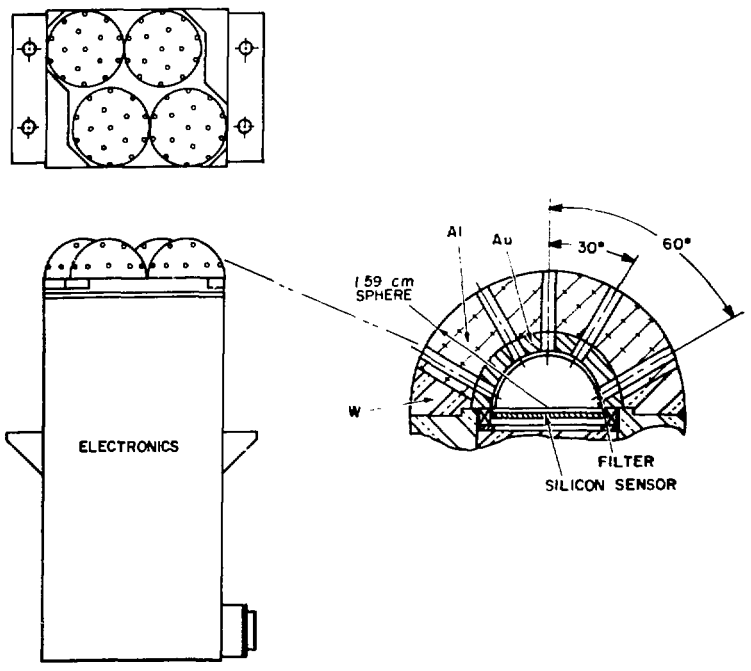

Fig. 1.
Simplified sketches of the BDD package and detector geometry.

TABLE I

DESIGN PARAMETERS OF THE FOUR BDD ENERGY CHANNELS

Filter Thickness[a] (mils)	Electron Threshold (MeV)	Proton Threshold (MeV)	Effective Solid Angle ($cm^2 \cdot sr$)	Estimated Electron Dose Rate[b] (MeV/s)	Maximum Proton Rate[c] (s^{-1})	Estimated Proton Dose Rate (MeV/s)
10	0.31	6	0.0029	29 000	510	32 000
25	0.57	10	0.00434	26 000	380	
60	1.05	17	0.00976	28 000	440	
135	1.45	27	0.0392	32 000	1190	

[a]Equivalent thickness of aluminum.
[b]As predicted by the model used by Roeske.
[c]For the 4-9 August 1972 solar proton event.

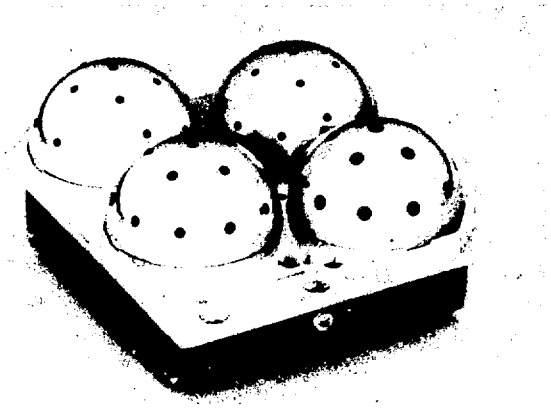

Fig. 2.
Photograph of the four BDD detectors.

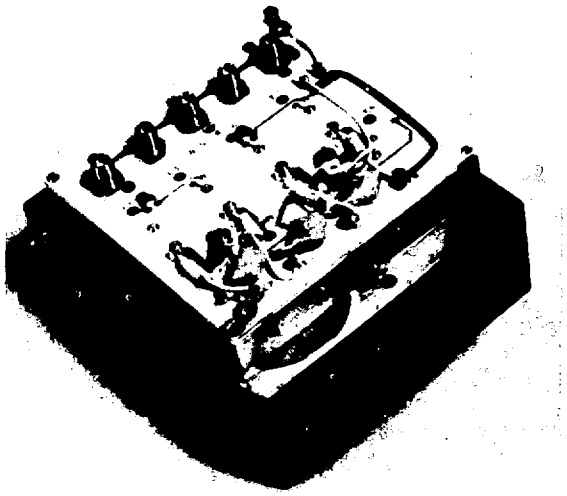

Fig. 3.
Photograph of the BDD electronics package.

Figure 4 shows two idealized sets of detector energy-response curves of the four channels, one for electrons and one for protons. The energy threshold of each channel is determined by the entrance-filter thickness. As the energy of the incident particle increases, the energy deposited in the sensor increases monotonically until the energy threshold for penetration of the sensor is reached. A sharp break in the energy deposition curve occurs at that energy, followed by a decrease as the energy of the particle approaches the minimum ionizing level. The maximum energy that an electron can deposit in the sensor is slightly greater than 0.4 MeV; the maximum energy deposited by a proton is approximately 10 MeV. An energy-level discriminator set near 0.5-0.6 MeV will effect separation of sensor pulses generated by electrons from those generated by protons with energies greater than 6 MeV. Since the electron fluxes are normally several orders of magnitude greater than the proton fluxes, there will be little contamination of the electron-flux data by protons with energies less than 0.5 MeV and no contamination of the proton-flux data by electrons.

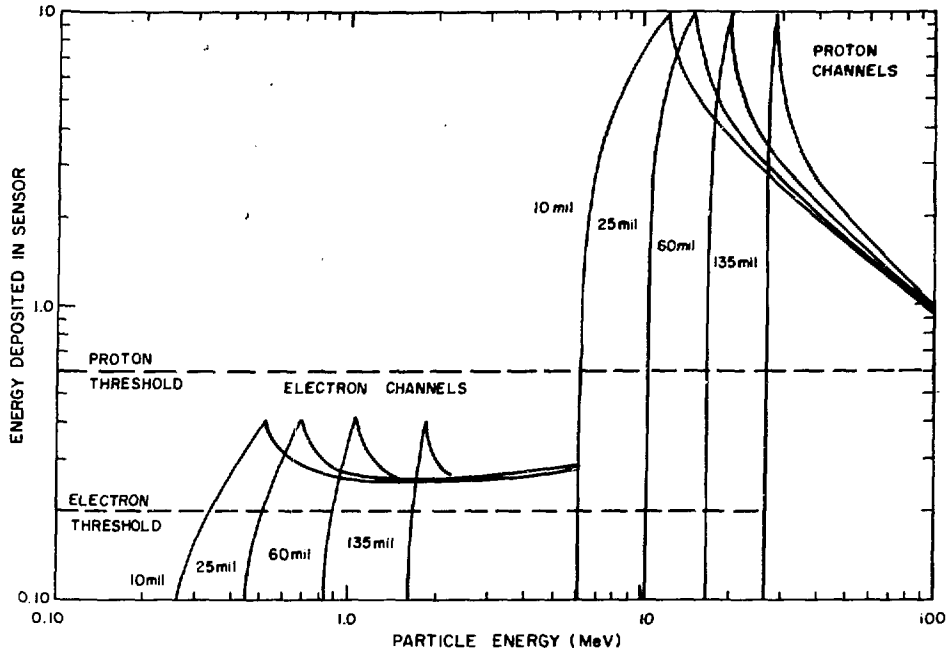

Fig. 4.
Idealized unit response functions for the four BDD channels. The thresholds are determined by the entrance filter thicknesses and the peaks by the sensor thickness.

Figure 5 shows examples of the electron and proton energy spectra that we expect to be encountered by the BDD. The particle fluxes are highly dependent on solar activity and will vary rapidly with position in orbit. The electron energy spectra are for equatorial orbits at an altitude of 11 000 nautical miles and are given by the AE-4 model of Singley and Vette[1] or by a calculation of Roeske* who used a preliminary version of the AE-7 model. The AE-4 10%-probability curve represents the electron energy spectrum that, according to this model, will be exceeded 10% of the time. The proton energy spectrum is that observed[2] during the giant solar proton events of 4-9 August 1972, which are the most intense high-energy proton fluxes ever recorded.

III. DATA ANALYSIS

Each channel will contain the integrated energy deposited by all electrons (protons) with energies greater than its electron (proton) threshold energy. The usual technique for converting observed count rates into fluxes[3] is to choose an effective energy threshold and a constant for the detector that minimize the effect of different energy spectra. Baker[4] and Van Allen *et al.*[5] gave a detailed exposition of this technique and coined for it the name "bow-tie analysis." In the case of regular spectra of the type encountered in magnctically trapped particle populations (Fig. 5), the technique can be applied to data taken over integrated energy intervals and can accurately reproduce the original spectrum.

The basis for this bow-tie analysis is the assumption that we can replace the relatively complex response function of a detector with a simple effective response function. As illustrated in Fig. 6a, we will replace the true response R(E) of a detector (solid curve) with an effective step-function response R* (dashed rectangular curve) characterized by the parameters ΔE^* (effective constant response) and E_T (effective threshold energy). That is, we will set

$$R(E) = 0 \quad \text{for } E < E_T$$

*These data were furnished by S. B. Roeske of Sandia Laboratories, Albuquerque.

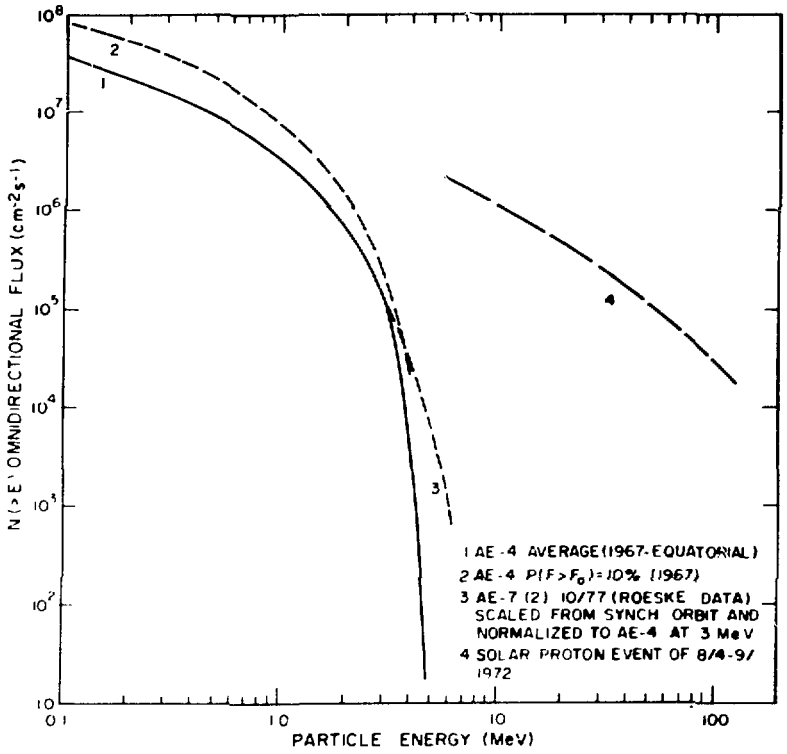

Fig. 5.
Energy spectra of trapped electrons at an altitude of 11 000 nautical miles as predicted by current models and of the giant solar proton event of 4-9 August 1972.

and

$$R(E) = \Delta E^* \text{ for } E \geq E_T \quad .$$

For each detector we will find an "optimum" parameter pair $(\Delta E^*, E_T)$ that will replicate its response over a wide range of incident-particle spectra.

To determine the optimum $(\Delta E^*, E_T)$, we establish the correspondence

$$\Delta E^* \int_{E_T}^{\infty} (dJ/dE)\, dE \rightleftarrows \int_{0}^{\infty} R(E)(dJ/dE)\, dE \quad . \quad (1)$$

The expression on the right is the exact count rate expected for an energy spectrum given by dJ/dE; it is determined by direct numerical integration of the product of the measured detector response R(E) and the energy spectrum dJ/dE. The expression on the left is the integral of the product of the step-function response and the energy spectrum. The electron spectra that we expect to be encountered by the BDD (Fig. 5) are well represented by an exponential form such as

$$dJ/dE \propto \exp(-E/E_0) \quad , \quad (2)$$

where $0.2 \text{ MeV} \leq E_0 \leq 1.0 \text{ MeV}$. Combining Eqs. 1 and 2 and expressing ΔE^* as a function of E_T, we obtain

$$\Delta E^* = \frac{\int_0^{\infty} R(E) \exp(-E/E_0)\, dE}{\int_{E_T}^{\infty} \exp(-E/E_0)\, dE} \quad . \quad (3)$$

Using Eq. 3, we then plot ΔE^* vs E_T for various values of the spectral index E_0; we obtain a family of curves that

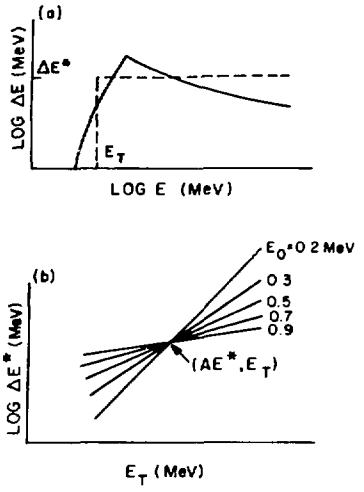

Fig. 6.

(a) Typical detector response function for an electron channel and the effective step-function response that is substituted for it in the bow-tie analysis.

(b) Family of curves obtained by plotting ΔE^* vs E_T for various values of the spectral index E_0. The coordinates $(\Delta E^*, E_T)$ of the point of intersection characterize an effective step-function response of the detector that accurately reproduces the original energy spectrum over a wide range of spectral indices.

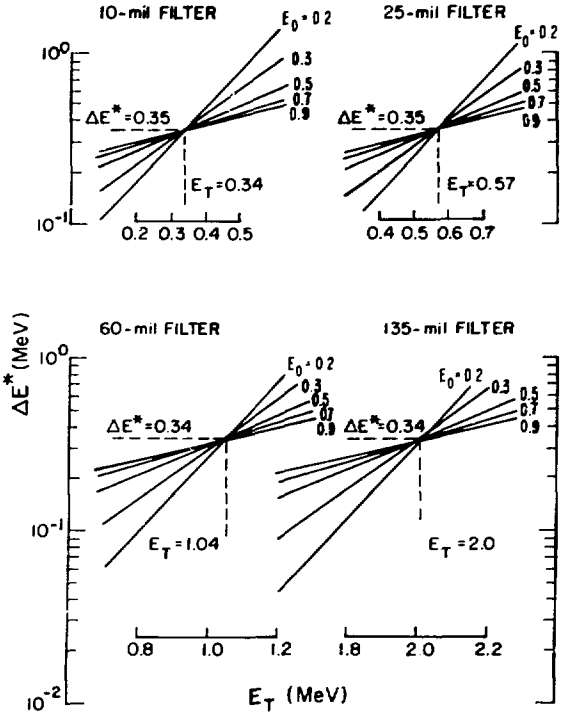

Fig. 7.

Results of bow-tie analyses for the four electron channels of the BDD.

roughly intersect at a point to form a bow tie, as illustrated in Fig. 6b. The average intersection point is assumed to be the optimum parameter pair $(\Delta E^*, E_T)$, which characterizes the effective response of the detector over a wide range of spectral indices. In the data analysis, the number of electrons in the spectrum above the threshold E_T is found by dividing the total energy deposited in the detector by the effective energy deposited per particle ΔE^*.

Figure 7 summarizes the bow-tie analysis results for the four electron channels of the BDD.

IV. DATA COLLECTION

Electrons and protons entering a detector through one of the collimating apertures will generate voltage pulses whose heights are proportional to the energy deposited in the sensor. The pulse height of each pulse (in MeV) is cumulatively stored in an appropriate eight-bit temporary-memory storage register of the BDD. There are eight such storage registers: four each for electron and proton pulse-height data. The pulses generated by electrons or protons are identified by pulse heights below or above, respectively, a predetermined level (~0.6 MeV).

Every 3.2 min the accumulated data in either the electron or proton storage registers is transferred and stored sequentially in the BDD portion of the BDP event memory. Every fourth time interval the BDD frame sync and satellite Z time are stored with the data. This block of data, four collection intervals plus Z time and frame sync, makes up a BDD data frame (BDDF) in event memory. A BDDF contains 24 eight-bit words; its detailed format is shown in Fig. 8.

The Z time is that of the immediately following BDD1. The BDD5X (X=A,B,C,D) are status words that indicate whether the data were generated by electrons or protons and specify the data collection mode and the upper and lower proton-rate thresholds.

There are three basic modes of data collection, selected by commutated XCAL1 command.

- 3/0 The electron channels are read out every 3.2 min.

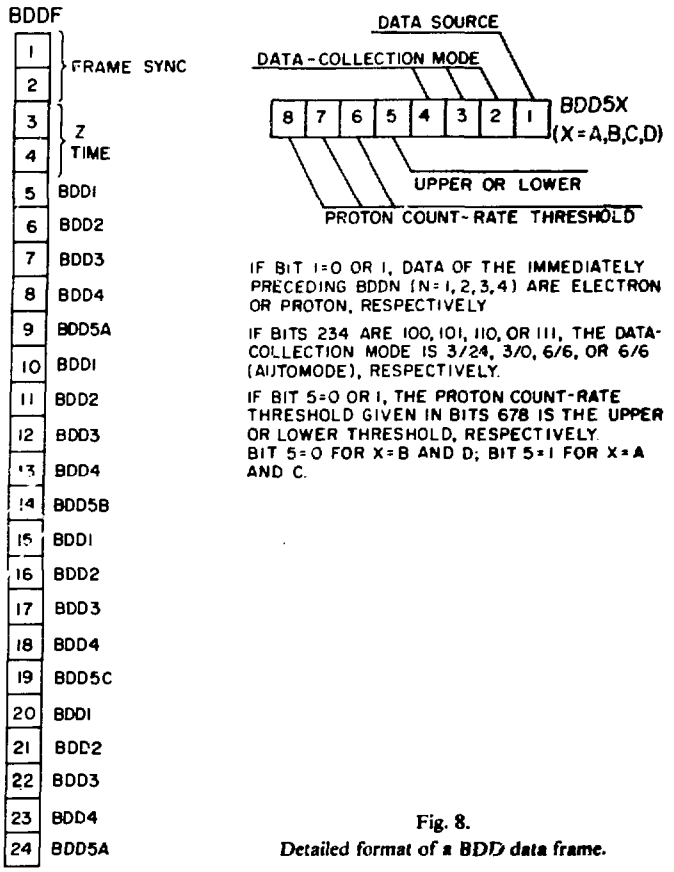

Fig. 8.
Detailed format of a BDD data frame.

- 6/6 The electron and proton channels are read out alternately every 3.2 min.
- 3/24 The electron channels are read out every 3.2 min for seven intervals; then the accumulated proton channels are read out at the end of the eighth interval.

Since there will be long periods during which the proton channels will be counting at or near background levels, the 3/0 and 3/24 modes will be used extensively. If a solar proton event should occur while data is being collected in either of these modes, circuitry is provided (see Sec. V) that will automatically change the data-collection mode. An upper proton-rate threshold, selected by commutated XCAL1 command from eight possible levels, effects a shift of the mode from 3/0 or 3/24 to 6/6 (automode) when the proton rate exceeds this threshold. A lower proton-rate threshold, again selected by commutated XCAL1 command from eight possible levels, effects return to the original mode when the proton rate falls below this threshold. Table II lists both the count rate and the accumulated count per 3.2 min interval associated with each of the eight upper and lower proton-rate thresholds.

The 4096 words of BDP event memory allocated for storage of BDDF will accommodate 36 h of data collection. It is planned to transmit the BDD data to ground on L3 every 24 h through an event memory readout.

V. CIRCUIT DESIGN

Figure 9 is a block diagram of the BDD circuits. The system consists of four surface-barrier silicon detectors with associated channels of analog electronics and data-handling logic. A detector pulse is amplified by a charge-sensitive preamplifier, which feeds in parallel an electron-level detector (ELD), a proton-level detector (PLD), and a pulse height-to-time converter that gates 4-MHz pulses, the number of which is proportional to the incident-particle energy.

TABLE II

PROTON COUNT-RATE THRESHOLDS

Threshold Designation	Upper Threshold		Lower Threshold	
	Accumulated Count per 3.2 min	Count Rate (s^{-1})	Accumulated Count per 3.2 min	Count Rate (s^{-1})
1	16 400	85	512	2.67
2	32 800	171	1 024	5.34
3	65 600	342	2 048	10.7
4	128 000	684	4 096	21.4
5	256 000	1 370	8 192	42.7
6	512 000	2 730	16 400	85.4
7	1 024 000	5 470	32 800	171
8	2 048 000	10 940	65 600	342

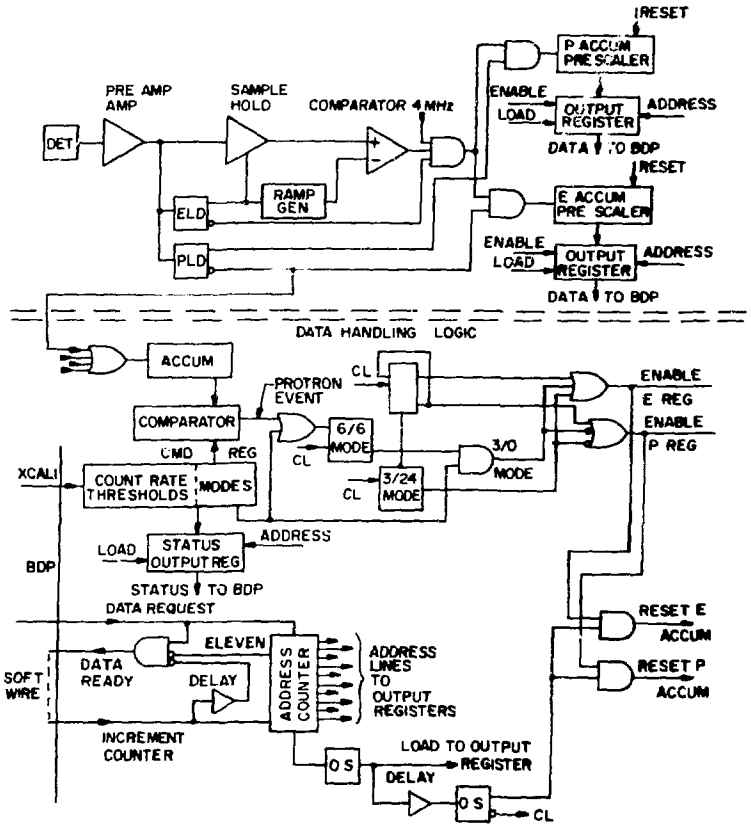

Fig. 9.
Block diagram of the BDD electronic circuits.

Triggering of the ELD upon receipt of a pulse inhibits the comparator gate and closes an analog switch to a sample-hold amplifier whose output is the positive input of the comparator. The negative input of the comparator is supplied by a ramp generator. A closed analog switch in the feedback path of the ramp generator results in a low gain (small positive voltage). The output of the comparator gate goes positive when the ELD pulse terminates, and the high comparator output initiates the gating of 4-MHz pulses. Absence of the ELD pulse opens the feedback path of the ramp generator and thus causes the gain to increase. The output of the ramp generator goes positive and is slowed by the charging of the feedback capacitor. At the point where the output of the ramp generator has gone as positive as the analog signal from the sample-hold amplifier, the output of the comparator goes to zero, and the 4-MHz gate is inhibited. The number of gated 4-MHz pulses is thus proportional to pulse height. If the amplifier pulse is large enough to trigger the PLD also, the electron 4-MHz gate is inhibited and the proton 4-MHz gate is enabled; the pulses are thus routed to the proton accumulator.

The output of the analog circuitry is a number of gated 4-MHz pulses on two lines, electron and proton, with the number of pulses proportional to the energy deposited in the detector. The digital circuitry accumulates these pulses, stores them until the BDP requests data (every 3.2 min), and then transfers them to BDP memory. The accumulated pulses are prescaled (bit-compressed—15 bits to 8 bits).

When data are requested by the BDP, the output register is read out, and the data currently being accumulated is shifted into temporary store in the output register. The accumulator is reset, and accumulation is started for the next time interval.

Data from all four proton channels are accumulated by a separate scaler and compared with a preselected upper count-rate threshold. If the proton count rate exceeds the selected level, the current data-collection mode is changed to 6/6 (automode). Data continue to be collected in this mode until the proton count rate falls below a preselected lower count-rate threshold; at this point, the data-collection mode is returned to the original mode. An eight-bit command register is incorporated in the system to enable selection of the data-collection mode and of the upper and lower proton count-rate thresholds.

REFERENCES

1. G. W. Singley and J. I. Vette, "The AE-4 Model of the Outer Radiation Zone Electron Environment," National Space Science Data Center report NSSDC 72-06 (August 1972).

2. J. H. King, "Solar Proton Fluences for 1977-1983 Space Missions," J. Spacecr. Rockets **11**, 401 (1974).

3. W. L. Kraushaar, G. W. Clark, G. P. Garmire, R. Borken, P. Higbie, C. Leong, and T. Thorsos, "High-Energy Cosmic Gamma-Ray Observations from the OSO-3 Satellite," Astrophys. J. **177**, 341 (1972).

4. D. N. Baker, "Energetic Particle Fluxes and Spectra in the Jovian Magnetosphere," Ph.D. thesis, University of Iowa, 1974.

5. J. A. Van Allen, D. N. Baker, B. A. Randall, and D. D. Sentman, "The Magnetosphere of Jupiter as Observed with Pioneer 10. 1. Instrument and Principal Findings," J. Geophys. Res. **79**, 3559 (1974).